LU TP 04-27

An improved algorithm for simulations of divergent-light halos

Lars Gislén, Jan O. Mattsson, and Bo Söderberg[*].

Divergent-light halos are produced when light from nearby light sources is scattered by ice crystals in the atmosphere. We present a theory of divergent-light halos leading to an improved algorithm for the simulation of such halos. Contrary to the algorithm we presented earlier for simulating such halos, the new algorithm includes a mathematically rigorous weighting of the events. The computer implementation is very compact and the whole procedure is elegant and conceptually easy to understand. We also present a new simulation atlas showing halos produced by crystals of different shapes and orientations for a set of elevations of the light source.

OCIS codes: 010.1290, 010. 2940, 010.3920

1. Introduction

In two earlier papers[1,2] we presented a new and efficient method for simulating divergent-light halos as well as comparisons with observations of such halos in the field. In these papers we also described the differences and similarities between ordinary parallel-light halos and divergent-light halos and explained why it is much more difficult to simulate a divergent-light halo than a parallel-light halo, a fact that explains why almost no such simulations have been published. For details we refer to our previous papers. Although the algorithm presented in these papers is computationally quite efficient it has draw-backs. The mathematics is somewhat involved and the computer program that implements the algorithm is lengthy and not very transparent. A more serious matter, as pointed out by Jarmo Moilanen[3], is that the algorithm lacks a proper event-weighting which, for instance gives a wrong intensity distribution in the divergent-light halo produced by randomly oriented ice crystals.

The present paper presents an improved algorithm that has a mathematically rigorous weighting of the events. Like the previous algorithm it is based on spatial rotations but instead of using a restricted set of rotations we now allow the full set of rotations in space. The algorithm is also much simpler, the computer implementation is very compact and the whole procedure is elegant and conceptually easy to understand.

2. Theory

2.1 Assumptions

Let the light source be located at the origin $\mathbf{O} = (0,0,0)$, and the observer at a fixed position **R** at a distance R from the origin. Let the cloud of ice crystals be characterized by a homogeneous number density *n* and a fixed distribution $Q(\mathbf{U})$ over possible crystal orientations, as given by applying a SO(3) rotation **U** to some standard orientation. Let the point-like light source have a total power *P*, isotropically radiated, and let *A* be the small aperture of the observer's eye. Assume the scattering by a single crystal to be described by a differential cross section $\frac{d\sigma}{d^2\hat{\mathbf{b}}}$, given an incident ray direction $\hat{\mathbf{a}}$, a scattered ray direction $\hat{\mathbf{b}}$, and a crystal orientation **U,**

[*] L. Gislén (LarsG@thep.lu.se) and B. Söderberg (Bosse@thep.lu.se) are with the Department of Theoretical Physics. J. O. Mattsson (Jan.Mattsson@nateko.lu.se)is with the Department of Physical Geography and Ecosystems Analysis, Lund University, Sweden.

where $\hat{\mathbf{a}}$ and $\hat{\mathbf{b}}$ are unit vectors. We express this cross section as a typical single crystal cross section σ_0 times a distribution over the scattered direction $p\left(\hat{\mathbf{b}} \mid \hat{\mathbf{a}}, \mathbf{U}\right)$, normalized such that

$$\int d^2\hat{\mathbf{b}}\, p\left(\hat{\mathbf{b}} \mid \hat{\mathbf{a}}, \mathbf{U}\right) = \sigma\left(\hat{\mathbf{a}}, \mathbf{U}\right)/\sigma_0 \sim 1. \tag{1}$$

We assume that the wavelength of the light is such that the scattering is accurately described by a ray-tracing model. We further assume that the scattering is rotationally covariant, i.e. it depends only on the relative orientations of the incoming and scattered radiation and the orientation of the crystal. This means that the distribution *p* is invariant under rotations,

$$p\left(\hat{\mathbf{b}} \mid \hat{\mathbf{a}}, \mathbf{U}\right) = p\left(\mathbf{U}^{-1}\hat{\mathbf{b}} \mid \mathbf{U}^{-1}\hat{\mathbf{a}}, \mathbf{U}^{-1}\mathbf{U}\right) = p\left(\mathbf{U}^{-1}\hat{\mathbf{b}} \mid \mathbf{U}^{-1}\hat{\mathbf{a}}, \mathbf{1}\right) \tag{2}$$

where **1** denotes the crystal in the standard orientation.

2.2 Halo distribution

If a crystal of orientation **U** is present at a position $\mathbf{a} = a\hat{\mathbf{a}},\ a = |\mathbf{a}|$, it experiences a light intensity (power/area) given by $I = P/\left(4\pi a^2\right)$. The total power scattered by the crystal is $P_s = I\sigma\left(\hat{\mathbf{a}}, \mathbf{U}\right)$, which is then distributed over different directions $\hat{\mathbf{b}}$ as $\sigma_0 I p\left(\hat{\mathbf{b}} \mid \hat{\mathbf{a}}, \mathbf{U}\right)$. The observer is located at **R**, i.e. at position $\mathbf{b} = \mathbf{R} - \mathbf{a}$ relative to the crystal, and sees only scattered rays coming in the direction $\hat{\mathbf{b}}$. Hence the intensity of the scattered radiation seen by the observer is $I_s = \sigma_0 I p\left(\hat{\mathbf{b}} \mid \hat{\mathbf{a}}, \mathbf{U}\right)/b^2$, which implies a total observed, scattered power per solid angle from the direction $-\hat{\mathbf{b}}$ given by $P_1 = AI_s$ or

$$P_1 = \frac{A\sigma_0 P}{4\pi a^2 b^2}\, p\left(\hat{\mathbf{b}} \mid \hat{\mathbf{a}}, \mathbf{U}\right) \tag{3}$$

Now, assume that the number density of crystals, *n*, be low enough such that

(i) the intensity *I* as described above does not noticeably diminish due to the scattering.
(ii) we can neglect multiple scattering.

Then we can simply sum the scattered power from all crystals, which means integrating over positions **a** with a factor *n*, and over orientations **U** with weight $Q(\mathbf{U})$. This yields, for the total power of scattered radiation that reaches the observer's eye, the expression

$$P_O = \frac{A\sigma_0 P n}{4\pi} \int \frac{d^3\mathbf{a}}{a^2 b^2} \int D\mathbf{U}\, Q(\mathbf{U}) p\left(\hat{\mathbf{b}} \mid \hat{\mathbf{a}}, \mathbf{U}\right) \tag{4}$$

The integration differential *D***U** represents the three parameters that describe the rotation **U**.

It appears natural to normalize this expression to the power P_{iso}, obtained by assuming that the scattering is completely isotropic and that the crystal orientations are random. This corresponds to $p\left(\hat{\mathbf{b}} \mid \hat{\mathbf{a}}, \mathbf{U}\right) = \dfrac{\sigma\left(\hat{\mathbf{a}}, \mathbf{U}\right)}{\sigma_0} \approx 1/4\pi$, yielding

$$P_{iso} = \frac{A\sigma_0 Pn}{4\pi^2}\int\frac{d^3\mathbf{a}}{a^2b^2}\int D\mathbf{U}\,Q(\mathbf{U}) = \frac{A\sigma_0 Pn}{4\pi^2}\int\frac{d^3\mathbf{a}}{a^2b^2} = \frac{A\sigma_0 Pn\pi}{4R} \tag{5}$$

Dividing the observed, scattered power P_O by P_{iso} gives a suitable expression for the observed scattered radiation

$$Z = \frac{4R}{\pi^2}\int\frac{d^3\mathbf{a}}{a^2b^2}\int D\mathbf{U}\,Q(\mathbf{U})p\left(\hat{\mathbf{b}}\,|\,\hat{\mathbf{a}},\mathbf{U}\right) \tag{6}$$

2.3 Bipolar angles and Minnaert's cigars

In the halo formalism it is convenient to introduce *bipolar angles* for parametrizing crystal positions in space. These bipolar angles are defined with respect to two points which we choose as **O** and **R**. Assume temporarily **R** to be along the positive *z* axis, i. e. $\mathbf{R} = (0,0,R)$. An arbitrary point in space (a crystal position), $\mathbf{a} = (x,y,z)$, can be expressed in bipolar angles ω, θ, and ϕ with respect to **O** and **R**, where θ and ϕ are usual polar angles with respect to **O**, while ω is defined by rewriting the radial coordinate *a* as

$$a = \frac{R\sin(\omega-\theta)}{\sin\omega} \tag{7}$$

and we obtain

$$\mathbf{a} = \frac{R\sin(\omega-\theta)}{\sin\omega}(\sin\theta\cos\phi,\sin\theta\sin\phi,\cos\theta) \tag{8}$$

with the ranges

$$\begin{aligned} &0 \le \theta \le \omega \le \pi \\ &0 \le \phi \le 2\pi \end{aligned} \tag{9}$$

Note that the complementary vector **b** from **a** to **R** becomes

$$\mathbf{b} = \mathbf{R} - \mathbf{a} = \frac{R\sin\theta}{\sin\omega}(-\sin(\omega-\theta)\cos\phi,-\sin(\omega-\theta)\sin\phi,\cos(\omega-\theta)) \tag{10}$$

The angle $\psi = \omega - \theta$ replaces the polar angle θ for **b**, and $\omega = \psi + \theta$ is the sum of the two polar angles, which is also the angle between **a** and **b**. A fixed value of ω defines a particular surface, a *Minnaert's cigar*[4] (fig. 1), which is parametrized by the polar angles θ and ϕ.For the geometry of such cigars see fig. 2 a, b.

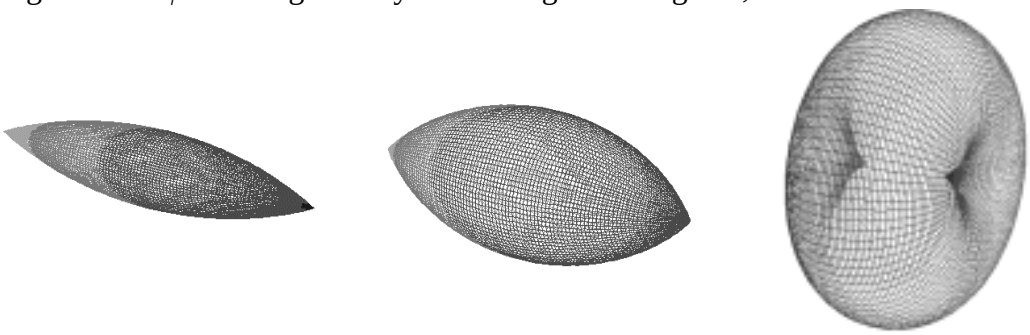

Figure 1a, b, c. Minnaert's cigars for scattering angles of 22˚, 45˚, and 150˚, respectively.

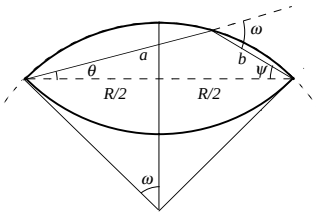

Figure 2a. Cigar geometry.

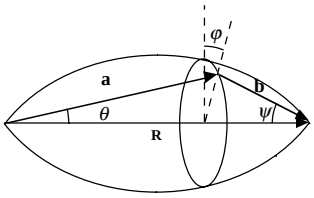

b. Locating a point on the cigar.

In particular note that the polar angles (ψ,φ) specify the apparent location of a crystal relative to the light source as seen by the observer (fig. 2 b).

The volume element becomes

$$d^3\mathbf{a} = R^3 \frac{\sin^2\theta \sin^2(\omega-\theta)}{\sin^4\omega} d\omega\, d\theta\, d\phi \qquad (11)$$

Since $a = R\sin(\omega-\phi)/\sin\omega$ and $b = R\sin\theta/\sin\omega$, this yields a very simple expression for the measure that appears in the halo distribution

$$\frac{d^3\mathbf{a}}{a^2b^2} = \frac{1}{R} d\omega\, d\theta\, d\phi \qquad (12)$$

2.4 Standard event distribution

When simulating a halo on a computer, the symmetry of the scattering distribution as expressed in (2) is very convenient. We wish to exploit this symmetry by reusing *standard events* by applying SO(3) rotations to them. A standard event is defined by having the crystal in a standard orientation (**U** = **1**), an incident ray with random direction $\hat{\mathbf{a}}_0$, and a direction $\hat{\mathbf{b}}_0$ in which light is scattered. The direction of scattering is found by ray-tracing the incident ray through the crystal until it exits. The *scattering angle*, $\omega = \arccos(\mathbf{a}_0 \cdot \mathbf{b}_0)$ is invariant under any rotation.

Only a two-dimensional manifold of rotated versions of a standard event is consistent with observability and constitute *observable events* – for a rotated standard event with a particular scattering angle ω to be observable, the crystal must be located on a particular Minnaert's cigar surface between the light source and the observer.

We need an expression for the distribution of a single, simulated standard event. A random incident direction corresponds to the measure $d^2\hat{\mathbf{a}}_0/4\pi$. The incident ray is made to randomly hit a disk perpendicular to $\hat{\mathbf{a}}_0$, with an area σ_0 large enough to contain the projection the crystal. A crystal in its standard orientation **U** = **1** yields for the direction of scatter, $\hat{\mathbf{b}}_0$, the distribution $p\left(\hat{\mathbf{b}}_0 \mid \hat{\mathbf{a}}_0, \mathbf{1}\right)$. Thus for all possible versions of events we get the integral

$$\int \frac{d^2\hat{\mathbf{a}}_0}{4\pi} \int d^2\hat{\mathbf{b}}_0 p\left(\hat{\mathbf{b}}_0 \mid \hat{\mathbf{a}}_0, \mathbf{1}\right) \le 1 \qquad (13)$$

The inequality appears because some incident rays will hit the disk outside the projection of the crystal. These events will be discarded.

In a computer simulation of a halo, a large number of standard events are produced, and the natural question is how to use them to compute *Z*, or rather $dZ/d^2\hat{\mathbf{b}}$, the halo intensity distribution.

2.5 Rewriting Z in terms of standard events

The previously computed expression for the properly normalized, observed scattering power can, using a Dirac delta function, be written

$$Z = \frac{4R}{\pi^2}\int\frac{d^3\mathbf{a}}{a^2}\int\frac{d^3\mathbf{b}}{b^2}\delta(\mathbf{a}+\mathbf{b}-\mathbf{R})\int D\mathbf{U}\,Q(\mathbf{U})p\left(\hat{\mathbf{b}}\,|\,\hat{\mathbf{a}},\mathbf{U}\right) \tag{14}$$

We want to rewrite this expression in terms of contributions from standard events $\left(\hat{\mathbf{a}}_0,\hat{\mathbf{b}}_0\right)$. This obviously requires rotations of the arguments of *p* in the integrand to the standard orientation. This means introducing rotated versions $\hat{\mathbf{a}}_0$ and $\hat{\mathbf{b}}_0$ of the real ray directions such that $\hat{\mathbf{a}}=\mathbf{U}\hat{\mathbf{a}}_0$ and $\hat{\mathbf{b}}=\mathbf{U}\hat{\mathbf{b}}_0$. To that end, we note that the integration over the the parameters of the SO(3) rotation **U** can be written as the integration over the pre-images, $\hat{\mathbf{a}}_0$, $\hat{\mathbf{b}}_0$, of the directions $\hat{\mathbf{a}}$, $\hat{\mathbf{b}}$, with a Dirac delta function securing the correct pair-wise scalar product, i. e.

$$D\mathbf{U} = d^2\hat{\mathbf{a}}_0 d^2\hat{\mathbf{b}}_0\delta\left(\hat{\mathbf{a}}_0\cdot\hat{\mathbf{b}}_0-\hat{\mathbf{a}}\cdot\hat{\mathbf{b}}\right) \tag{15}$$

This yields, using the symmetry (2) of *p*,

$$Z = \frac{4R}{\pi^2}\int\frac{d^3\mathbf{a}}{a^2}\int\frac{d^3\mathbf{b}}{b^2}\delta(\mathbf{a}+\mathbf{b}-\mathbf{R})\int d^2\hat{\mathbf{a}}_0 d^2\hat{\mathbf{b}}_0\delta\left(\hat{\mathbf{a}}_0\cdot\hat{\mathbf{b}}_0-\hat{\mathbf{a}}\cdot\hat{\mathbf{b}}\right)Q(\mathbf{U})p\left(\hat{\mathbf{b}}_0\,|\,\hat{\mathbf{a}}_0,\mathbf{1}\right) \tag{16}$$

After some reordering this can be written in the convenient form

$$Z = \int\frac{d^2\hat{\mathbf{a}}_0}{4\pi}\int d^2\hat{\mathbf{b}}_0\; p\left(\hat{\mathbf{b}}_0\,|\,\hat{\mathbf{a}}_0,\mathbf{1}\right)W\left(\hat{\mathbf{a}}_0,\hat{\mathbf{b}}_0\right) \tag{17}$$

i.e. as an integration over standard events $\left(\hat{\mathbf{a}}_0,\hat{\mathbf{b}}_0\right)$ with one weight factor *p* that handles the outcome of the ray-tracing and a second weight factor *W*, representing their total contribution to *Z*, which is

$$W\left(\hat{\mathbf{a}}_0,\hat{\mathbf{b}}_0\right) = \frac{16}{R}\int\frac{d^3\mathbf{a}}{a^2}\int\frac{d^3\mathbf{b}}{b^2}\delta(\mathbf{a}+\mathbf{b}-\mathbf{R})\,\delta\left(\hat{\mathbf{a}}_0\cdot\hat{\mathbf{b}}_0-\hat{\mathbf{a}}\cdot\hat{\mathbf{b}}\right)Q(\mathbf{U}) \tag{18}$$

Here, **U** is seen as depending on $\hat{\mathbf{a}}$, $\hat{\mathbf{b}}$, $\hat{\mathbf{a}}_0$, and $\hat{\mathbf{b}}_0$. Explicitly we have

$$\mathbf{U} = \frac{\hat{\mathbf{a}}\hat{\mathbf{a}}_0^{\mathrm{T}}+\hat{\mathbf{b}}\hat{\mathbf{b}}_0^{\mathrm{T}}-\cos\omega\left(\hat{\mathbf{a}}\hat{\mathbf{b}}_0^{\mathrm{T}}+\hat{\mathbf{b}}\hat{\mathbf{a}}_0^{\mathrm{T}}\right)+\left(\hat{\mathbf{a}}\times\hat{\mathbf{b}}\right)\left(\hat{\mathbf{a}}_0\times\hat{\mathbf{b}}_0\right)^{\mathrm{T}}}{\sin^2\omega} \tag{19}$$

where the vectors are considered to be column matrices and the superscript "T" denotes matrix transpose.

The expression for *W* suggests that bipolar angles would be convenient, yielding

$$W = \frac{16}{\pi}\int_0^{\pi}d\omega\int_0^{\omega}d\theta\int_0^{2\pi}d\phi\,\delta\left(\cos\omega-\hat{\mathbf{a}}_0\cdot\hat{\mathbf{b}}_0\right)Q(\mathbf{U}) \tag{20}$$

The Dirac delta function fixes the value of ω and thus a definite cigar, as is to be expected; a rotation of the directions $\hat{\mathbf{a}}_0$ and $\hat{\mathbf{b}}_0$ cannot change their relative angle. Eliminating the ω integral gives a very simple expression for the event weight:

$$W = \frac{32\omega}{\sin\omega}\int_0^{\omega}\frac{d\theta}{\omega}\int_0^{2\pi}\frac{d\phi}{2\pi}\,Q(\mathbf{U}) \tag{21}$$

where now **U** is to be regarded as a function of ω, θ, and ϕ. The weight is evenly distributed over cigar angles θ and ϕ, apart from the factor $Q(\mathbf{U})$, which modifies the weight distribution depending on the crystal orientation associated with a particular point on the cigar.

The weight distribution is seen to decompose into two parts, the intrinsic *cigar weight* that is proportional to $\frac{\omega}{\sin\omega}$, and the factor $Q(\mathbf{U})$ which modifies the uniform cigar measure $\frac{d\theta}{\omega}\frac{d\varphi}{2\pi}$ by suppressing points on the cigar that correspond to less probable crystal orientations.

We see that effectively we have split the halo intensity distribution into three factors: one describing a single crystal scattering in a standard crystal frame, another that gives the associated intensity contribution to the weight for isotropic crystal orientations, and finally one that takes into account the actual distribution of crystal orientations. This factorization is not unique but turns out to be convenient for the implementation of our computer algorithm.

3. Implementation

The algorithm we use can be summarized as follows:

1) Assume a standard orientation the crystal such that the main axis of the crystal is in the *z* direction (vertical), and one of the crystal side faces is parallel to the *xz* plane. This defines the standard frame **U** = **1**. Generate a random incident ray, ray-trace it through the crystal to get a scattered ray. The directions of the incident and scattered rays $\left(\hat{\mathbf{a}}_0,\hat{\mathbf{b}}_0\right)$, then completely specify the event, given the standard orientation of the crystal.

2) The scattering angle $\omega = \arccos\left(\hat{\mathbf{a}}_0 \cdot \hat{\mathbf{b}}_0\right)$ defines a specific Minnaert's cigar with its axis pointing away from the light source at **O** towards the observer at **R**. The contribution weight of an event with a scattering angle ω is proportional to $\omega/\sin\omega$. We implement this weight by reusing each standard event a number of times that is proportional to this weight, where we have normally chosen the proportionality factor *K* = 20. The choice of the factor *K* requires some experimentation. If $Q(\mathbf{U})$ is narrow, this factor may be set fairly large in order to reduce computation time. In the opposite case, as in the case of a random orientation of the crystals, a too large factor will "overexpose" the halo display.

3) For each usage of a standard event, select a point on the cigar by randomly choosing polar angles θ in the interval $[0,\omega]$ and φ in $[0,2\pi]$. This implements the measure $\frac{d\theta}{\omega}\frac{d\varphi}{2\pi}$. Note that the random choice of θ is equivalent of choosing the observer's polar angle ψ randomly in $[0,\omega]$. Given the vector **R** from the light source to the observer, the polar angles uniquely determine the rotation **U** that gives the orientation of the crystal for the observable event.

4) We finally determine the value of $Q(\mathbf{U})$ associated with the actual rotated crystal orientation and plot a point in the sky in the reverse direction $-\hat{\mathbf{b}}(\psi,\phi)$ of the scattered ray with a probability proportional to this value.

The weight $\omega/\sin\omega$ diverges for back-scattering, $\omega=\pi$. Such events, as seen by the observer, are either concentrated in the direction of the light source or in the opposite direction or correspond to rays scattered by crystals very far away. The divergence is a consequence of our approximation being valid only for crystal distances that are small compared to the mean free path. We handle this divergence by setting the weight for scattering angles larger than 179˚ equal to the weight at 179˚.

4. A limiting case

The model here also allows us to describe and simulate what happens when the distance between the light source and the observer is very large. This will reduce the influence of parts of the Minnaert's cigar that are far from the observer. There could be several reasons for this:

1) The cloud of ice crystals is finite in extension.
2) Rays from distant crystals are absorbed by the air. There is also an intensity threshold for the eye below which it will not register light.
3) Double scattering and defects, particularly in smaller crystals, will spread the rays away from the original, single scattering direction.
4) Possibly diffractive effects could, for very small crystals, also spread the light and diminish the light intensity.

A simple way to simulate the distance dependence is to cut away more distant parts of the cigar by generating points on the cigar only within a small sphere of radius *r*, centered at the position of the observer. A light source at infinite distance then corresponds to letting this radius going to zero. Simple geometrical considerations (see fig. 3) imply that if we assume $r << R$ we have for expression (19)

$$W=\frac{32\omega}{\sin\omega}\int_0^{\arcsin\left(\frac{r}{R}\sin\omega\right)}\frac{d\theta}{\omega}\int_0^{2\pi}\frac{d\varphi}{2\pi}\,Q(\mathbf{U})\approx \tag{22}$$

$$\frac{32\omega}{\sin\omega}\int_0^{\frac{r}{R}\sin\omega}\frac{d\theta}{\omega}\int_0^{2\pi}\frac{d\varphi}{2\pi}\,Q(\mathbf{U})\overset{h=\frac{r}{R}\sin\omega}{=}\frac{32r}{R}\int_0^1 dh\int_0^{2\pi}\frac{d\varphi}{2\pi}\,Q(\mathbf{U})$$

Thus in the limiting case of an infinite distance to the source (parallel-light halo) the cigar weight is independent of the scattering angle ω. We have used this as a convenient way of checking the simulation and to verify that we recover the ordinary parallel-light halos as $r\to 0$.

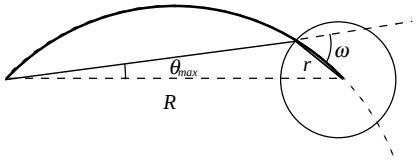

Figure 3. Restricting the cigar to crystals located close to the observer. If $r < R$ we have $\theta_{max}=\arcsin\left(\frac{r}{R}\sin\omega\right)$.

5. New results

We give a new version of the fisheye atlas for oriented plate (fig. 4) and singly-oriented column crystals (fig. 5) for source elevations from 10˚ to 60˚, and also for Parry-oriented crystals (fig. 6). The oriented plate crystals have an axis tip angle of

1.0˚ from the vertical and a c/a ratio of 0.3. The column crystals have an axis tip angle of 0.5˚ from the horizontal and a c/a ratio of 2.0. For the Parry arcs we assumed that the normal of a side face of the crystal had a tip angle of 1.5˚ from the vertical and that the crystal had a c/a ratio of 2.0. The distribution in tip angle is a Gaussian distribution with zero mean and a standard deviation equal to the tip angle. The c/a ratio is defined conventionally as the ratio between the distance across a basal face of a crystal and the distance between the basal faces.

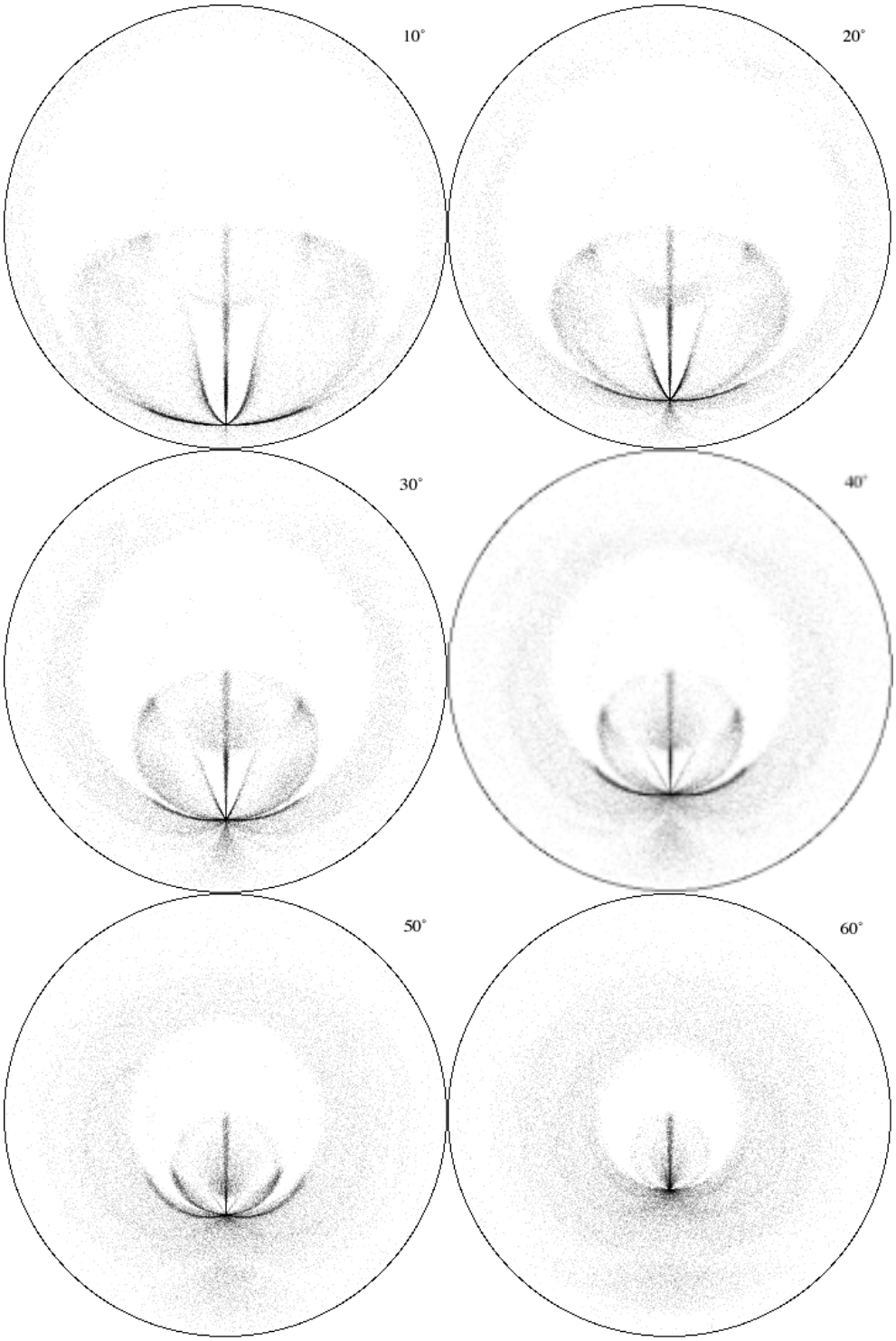

Figure 4. Atlas for oriented plate crystals.

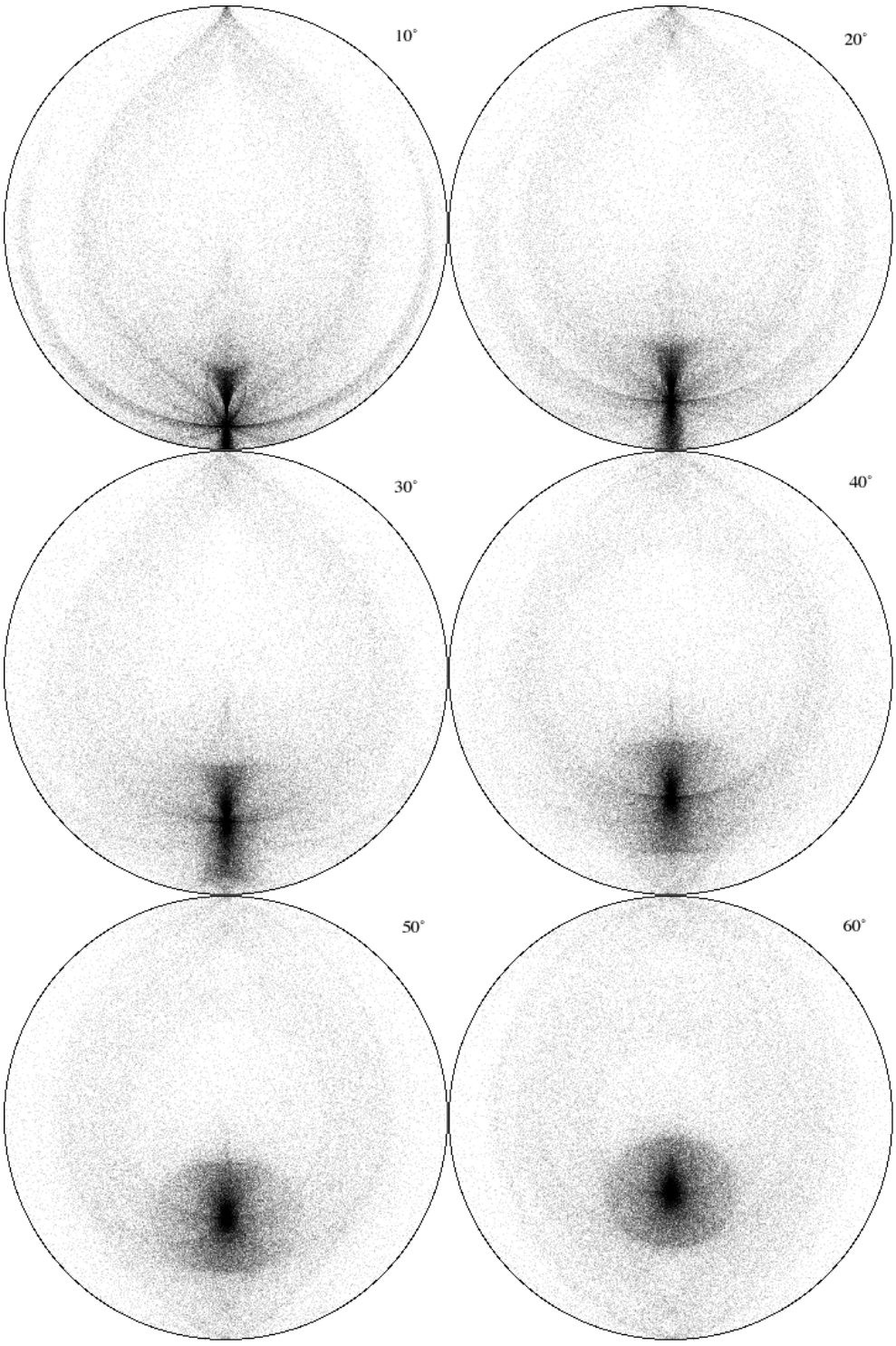

Figure 5. Atlas for singly-oriented column crystals.

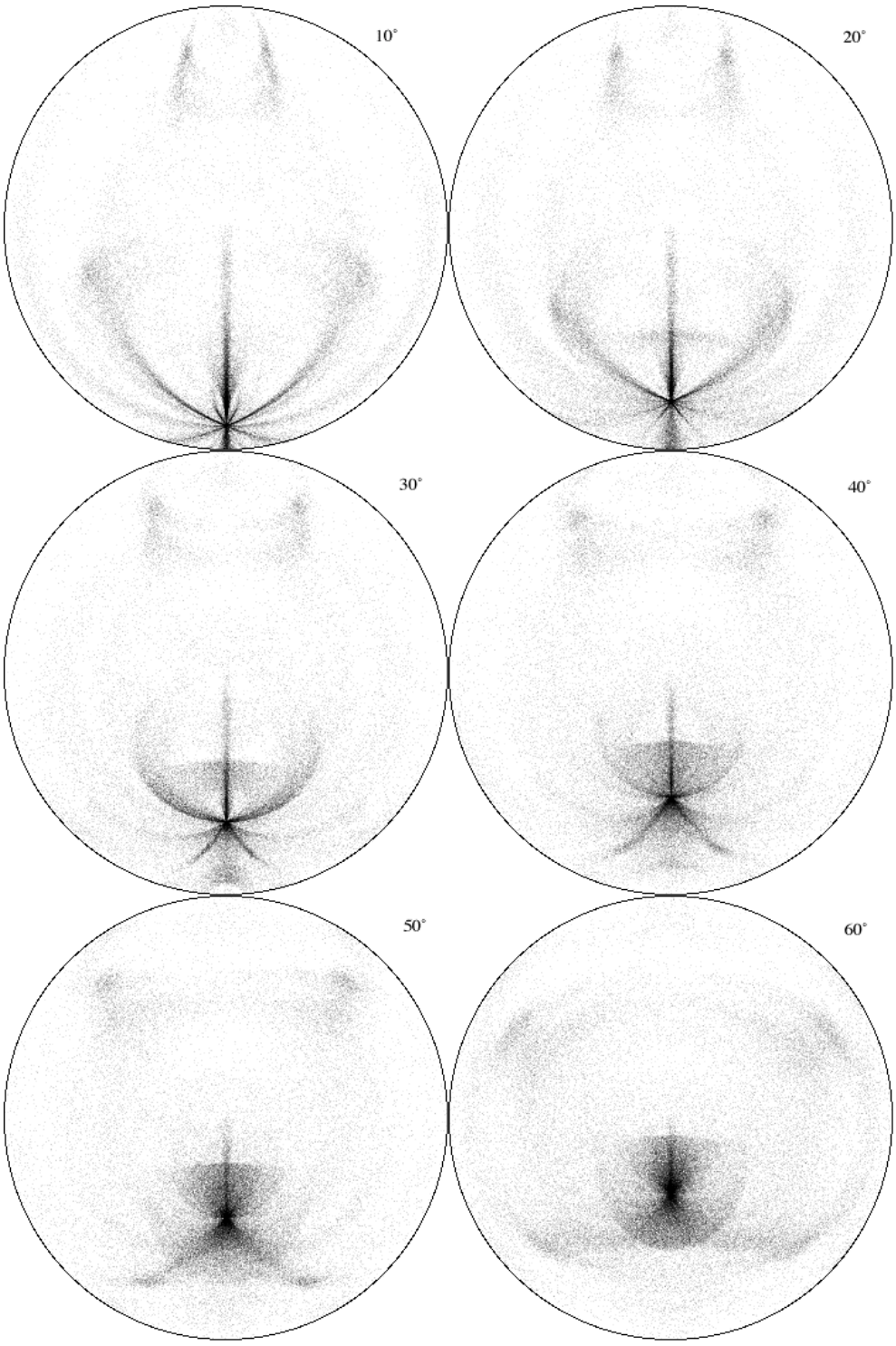

Figure 6. Atlas for Parry-oriented crystals.

6. Discussion

The halos in the atlas formed by oriented plate crystals (fig. 4) are in shape and size similar to the corresponding halos given in our earlier simulations[1]. Strong, well-developed superparhelia stretch out obliquely and upwards from the source at lower elevations. There is also a weak parhelic circle. A bright, well-defined light pillar appears not only at lower light elevations but also at high elevations. A distinct part of the parhelic circle reveals the 22˚ parhelia streching horizontally inwards to the source. The faint arcs of the 120˚ parhelia can still be seen for higher source elevations in the new atlas, albeit weaker than before. The circumzenithal as well as the circumhorizontal arcs are less distinct in the new atlas but otherwise similar to their presentations given in the earier version of the atlas. New and very interesting features are the arcs and bright spots appearing between the parhelic circle and the superparhelia. These are due to crystals where the ray enters one of the side faces, makes an odd number of reflections in the end faces and exits through a side face as illustrated in fig. 7.

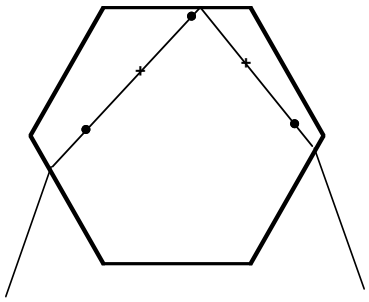

Figure 7. Path of reflected light within a crystal. Dots and crosses represent reflections in the upper and lower endfaces, respectively.

For a crystal with a vertical main axis this ray path will be horizontally equivalent to a reflexion in a vertical mirror and vertically the ray will be scattered back in the opposite direction. These features are located behind the light source as seen by the observer. This can be seen in fig. 8 where we have excluded rays from the souce in the backward hemisphere and these arcs then practically disappear. Note that features associated with crystals behind the light source are unique for divergent-light halos, and obviously they cannot be present in a solar halo.

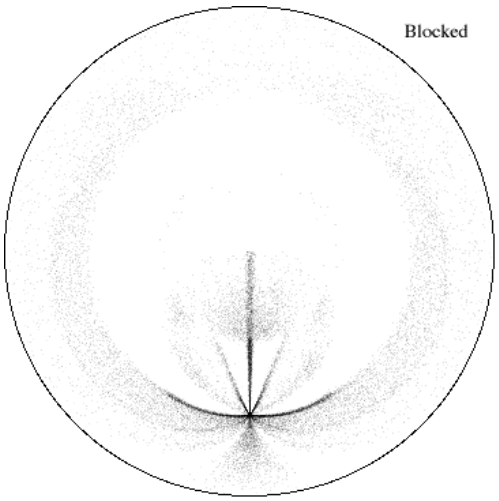

Figure 8. Halo produced by oriented plate crystals for a light source elevation of 30˚, where the rays in the rear hemisphere of the light source (behind the lamp) has been blocked out.

The halos in the atlas formed by singly-oriented column crystals (fig. 5) also resemble corresponding halos in our earlier atlas, albeit more blurred than these. The upper and lower tangent arcs and their transformation at high source elevations into a circumscribed halo are still discernible. Halo arcs for this category of crystals, which were not so evident in the former atlas presentation, are a well-developed parhelic circle and, for lower source elevations, traces of superparhelia. A faint anthelion connected to a diffuse area is also discernible for lower elevations.

Halos formed by Parry-oriented crystals in divergent light (fig. 6), are also presented in the new atlas. They include theoretically expected but probably extremely rare halos. Due to the more restricted orientation of the crystals, the halo patterns have more in common with the parallel-light halo patterns. We can for example see traces of the antisolar arc and the heliac arc and, for higher source elevations, also the upper and lower suncave arcs.

7. Final remarks

The statement in the final remarks of our earlier study[1], namely, that the simulation model is very idealized, is still valid. Perfect hexagonal crystals homogeneously distributed in an unlimited space of air, and unobstructed light from a point-like light source are thus still assumed. In many cases in the field, the rays from the light-source (a street-lamp) are substantially restricted by a lamp-shade which, as we have seen, can alter the halo display substantially.

We hope that the improved algorithm for divergent-light halo simulation presented here will stimulate the studies of these nocturnal ”close-to-the-eye” halos, but we also stress the need in field observations of including, wherever possible, photographic documentation of the phenomena and of specifying the degree of isotropy of the light source. A verification of the arcs behind the lamp produced by oriented plate crystals that are predicted by the simulations would also be of great interest.

A beta version of the algorithm unit is available at http://www.thep.lu.se/~larsg/ .

We are greatly indebted to Jarmo Moilanen for critical comments leading to this paper.

Appendix

If we assume isotropic scattering in a cloud with a large but finite radius r of randomly oriented crystals, the total scattered power (observed or not) is

$$P_{tot} = \frac{Pn\sigma_0}{4\pi}\int \frac{d^3\mathbf{a}}{a^2} = Pn\sigma_0 r \qquad (23)$$

The mean free path is $d = 1/(n\sigma_0)$ which yields

$$P_{tot}/P = r/d \qquad (24)$$

Clearly for our approximation assumptions to be valid, this ratio should be much less than 1, i.e. $r << d$.

It is also interesting to note that for isotropic scattering of randomly oriented crystals the halo distribution $dZ/d^2\hat{\mathbf{b}}$ is very simple, given by

$$\frac{dZ}{d^2\hat{\mathbf{b}}} = \frac{R}{\pi^3}\int_0^\infty \frac{db}{\left(\mathbf{R} - b\hat{\mathbf{b}}\right)^2} = \frac{\pi - \psi}{\pi^3 \sin\psi} \qquad (25)$$

Here $\psi = \arccos\left(\hat{\mathbf{R}} \cdot \hat{\mathbf{b}}\right) = \omega - \theta$ is the previously defined polar angle of the location of crystal as senn by the observer. $dZ / d^2\hat{\mathbf{b}}$ is a smooth distribution over directions, which however diverges for $\psi \to 0$, i.e. for the part of the halo close to the light source.

References

1. L.Gislén, J. O. Mattsson, *"Observations and Simulations of Some Divergent-Light Halos"*, Appl. Opt., 42, 4269-4279, (2003)
2. L.Gislén, *"Procedure for Simulating Divergent-Light Halos"*, Appl. Opt., 42, 6559-6563, (2003)
3. Private communication.
4. J. O. Mattsson, L. Bärring, and E. Almqvist, *"Experimenting with Minnaert's Cigar"*, Appl. Opt., 39, 3604-3611, (2000)